

# Transglutaminase 6: a protein associated with central nervous system development and motor function

Helen Thomas · Konrad Beck · Magdalena Adamczyk ·  
Pascale Aeschlimann · Martin Langley · Radu C. Oita ·  
Lars Thiebach · Martin Hils · Daniel Aeschlimann

Received: 28 June 2011 / Accepted: 16 September 2011 / Published online: 8 October 2011  
© The Author(s) 2011. This article is published with open access at Springerlink.com

**Abstract** Transglutaminases (TG) form a family of enzymes that catalyse various post-translational modifications of glutamine residues in proteins and peptides including intra- and intermolecular isopeptide bond formation, esterification and deamidation. We have characterized a novel member of the mammalian TG family, TG6, which is expressed in a human carcinoma cell line with neuronal characteristics and in mouse brain. Besides full-length protein, alternative splicing results in a short variant lacking the second  $\beta$ -barrel domain in man and a variant with truncated  $\beta$ -sandwich domain in mouse. Biochemical data show that TG6 is allosterically regulated by  $\text{Ca}^{2+}$  and guanine nucleotides. Molecular modelling indicates that TG6 could have

$\text{Ca}^{2+}$  and GDP-binding sites related to those of TG3 and TG2, respectively. Localization of mRNA and protein in the mouse identified abundant expression of TG6 in the central nervous system. Analysis of its temporal and spatial pattern of induction in mouse development indicates an association with neurogenesis. Neuronal expression of TG6 was confirmed by double-labelling of mouse forebrain cells with cell type-specific markers. Induction of differentiation in mouse Neuro 2a cells with NGF or dibutyryl cAMP is associated with an upregulation of TG6 expression. Familial ataxia has recently been linked to mutations in the TGM6 gene. Auto-antibodies to TG6 were identified in immune-mediated ataxia in patients with gluten sensitivity. These findings suggest a critical role for TG6 in cortical and cerebellar neurons.

H. Thomas and K. Beck contributed equally to this work.

**Electronic supplementary material** The online version of this article (doi:10.1007/s00726-011-1091-z) contains supplementary material, which is available to authorized users.

H. Thomas · K. Beck · M. Adamczyk · P. Aeschlimann ·  
M. Langley · R. C. Oita · D. Aeschlimann (✉)  
Matrix Biology and Tissue Repair Research Unit,  
School of Dentistry, Cardiff University, Heath Park,  
Cardiff CF14 4XY, UK  
e-mail: AeschlimannDP@Cardiff.ac.uk

M. Adamczyk · P. Aeschlimann  
Arthritis Research UK Biomechanics and Bioengineering  
Centre, Cardiff University, 51 Park Place,  
CF10 3AT Cardiff, UK

L. Thiebach  
Institute for Biochemistry, Medical Faculty,  
University of Cologne, Joseph-Stelzmann Str. 52,  
50931 Cologne, Germany

M. Hils  
ZEDIRA, Roesslerstr. 83, 64293 Darmstadt, Germany

**Keywords** Transglutaminase 6 · Sequence · Structural model · Regulation · Central nervous system · Ataxia

## Abbreviations

CNS	Central nervous system
DIG	Digoxigenin
GFAP	Glial fibrillary acidic protein
HD	Huntington's disease
PCR	Polymerase chain reaction
RT	Reverse transcription
SCA	Spinocerebellar ataxia
TG	Transglutaminase

## Introduction

Transglutaminases (TG) are a family of structurally and functionally related enzymes that post-translationally modify proteins by catalysing a  $\text{Ca}^{2+}$ -dependent transferase reaction between the  $\gamma$ -carboxamide group of a

peptide-bound glutamine residue and various primary amines. Most commonly, intra- or intermolecular  $\gamma$ -glutamyl- $\epsilon$ -lysine crosslinks are formed by reaction with the  $\epsilon$ -amino group of a lysine residue (Folk and Chung 1973). The action of these enzymes consequently results in the formation of covalently crosslinked, often insoluble supra-molecular structures and has a well-established role in tissue homeostasis in many biological systems (Aeschlimann and Thomazy 2000; Lorand and Graham 2003; Iismaa et al. 2009). Besides crosslinking, peptide-bound glutamine residues may be modified by TG through reaction of the acyl-enzyme intermediate with low-molecular-weight metabolites harbouring amino groups, or through hydrolysis or esterification. Conversion through hydrolysis is comparably slow and occurs preferentially at pH < 6.5. Nevertheless, the biological significance of enzymatic deamidation of glutamine has been illustrated by its role in T-cell activation in celiac disease (Molberg et al. 1998; Van de Wal et al. 1998). Transamidation has profound effects on the biological activity of many substrate proteins and it has become clear that some TGs preferentially form intermolecular crosslinks, whereas others catalyse primarily intramolecular reactions (Candi et al. 1995). Such protein modifications can be dynamic as conversion of the acyl-enzyme intermediate to the isopeptide bond is reversible (Parameswaran et al. 1997). TGs are evolutionarily related to papain-like cysteine proteases, both in terms of the structure of the core domain and the mechanism of catalysis, and more distantly to the peptide *N*-glycanases. Other enzymes have evolved in lower species that can catalyse the same transamidation reaction. These, however, bear no genetic relationship to the TG genes in man and the mechanism of catalysis is distinct, although it depends on a reactive thiol in the enzyme active site. These include *Streptomyces* microbial TG, bacterial toxins (including cytotoxic necrotizing factor from *E. coli* and dermonecrotic toxin from *Bordetella*), and thioredoxin/protein-disulfide isomerase-like enzymes from primitive eukaryotes (e.g. ERp60-like from nematodes and PDI from *Giardia*).

Nine different TG genes have been characterized in mammals (Aeschlimann and Paulsson 1994; Aeschlimann et al. 1998; Grenard et al. 2001). They exhibit a similar overall organization, with remarkable conservation of intron distribution and intron splice types. Detailed comparison of the structure of the individual genes shows that they may be divided into two subclasses, wherein the TGM2-7 and EBP42 genes contain 13 exons, and the F13A1 and TGM1 genes contain 15 exons (Grenard et al. 2001). Exon 9 of the former group is separated into two exons, 10 and 11, in the TGM1 and F13A1 genes, and the non-homologous *N*-terminal extensions of factor XIII a-subunit and TG1 that are absent in other TGs are comprised by an additional exon. Several TG gene products

have been characterized in detail using a combination of mutagenesis and structural studies to elucidate the enzymatic mechanism and its regulation. The three-dimensional structures of three TGs have been solved, i.e. factor XIII a (Yee et al. 1994), TG2 (Liu et al. 2002) and TG3 (Ahvazi et al. 2002). All comprise of four domains that are similar in organization: an amino terminal  $\beta$ -sandwich domain which forms a functional unit with the core domain; the catalytic core domain that contains the conserved active site triad cysteine, histidine and aspartate residues; and two *C*-terminal  $\beta$ -barrel domains which are involved in the regulation of enzyme activity. Molecular modelling and docking studies on TG3 proposed that binding of two additional  $\text{Ca}^{2+}$  ions converts the enzyme to the active form on the approach of the first substrate (glutamine-containing polypeptide) (Ahvazi et al. 2004). A recent X-ray structure of a trapped transamidation intermediate of TG2 (Pinkas et al. 2007) explained for the first time how a crosslinked protein complex could be released from the enzyme after catalysis as well as the considerable increase in radius of gyration observed by small-angle X-ray scattering for activated TG2 in solution (Mariani et al. 2000). TG2 undergoes a large conformational change whereby the  $\beta$ -barrel domains are rotated almost 180° into the plane of the other two domains, thereby exposing the enzyme active site (Pinkas et al. 2007).

TGs have been implicated in the pathogenesis of several neurodegenerative diseases (polyglutamine expansion diseases, Alzheimer's, Parkinson's and supranuclear palsy), but despite extensive investigation over at least two decades ambiguity remains as to the physiological function of TGs in the central nervous system (CNS) as well as their role in pathogenesis (for review see Iismaa et al. 2009; Jeitner et al. 2009). It has been shown that pathological length CAG expansions are excellent substrates for TG2 and that TG2 activity is increased in the brains of patients with Huntington's disease (HD) and certain forms of spinocerebellar ataxia (SCA) (Lesort et al. 1999). In Alzheimer's disease TGs have been localised to plaques and tangles and these contain substrates of TG2 (Kim et al. 1999). Similarly, the presence of TG crosslinked  $\alpha$ -synuclein in substantia nigra dopaminergic neurons of Parkinson's disease patients has been demonstrated (Andringa et al. 2004). The fact that increased levels of the  $\gamma$ -glutamyl- $\epsilon$ -lysine crosslink as well as *bis*- $\gamma$ -glutamylpolyamine are found in the affected tissue and in the cerebrospinal fluid (Zainelli et al. 2003; Nemes et al. 2004; Jeitner et al. 2008) indicates that TG2 and possibly other TG isozymes extensively modify proteins and possibly also disease-specific protein aggregates. Mouse models have substantiated a direct role of TG2 in the pathogenesis of Huntington's and other neurodegenerative diseases albeit the mechanisms involved being somewhat unexpected. HD

mice (R6/1 and R6/2) lacking TG2 exhibit delayed mortality and behavioural deficits but have increased aggregate formation (Mastroberardino et al. 2002; Bailey and Johnson 2005). It is therefore possible that TG2 contributes to the pathogenesis by modulating the size of the aggregates formed, leading to the formation of smaller aggregates (Lai et al. 2004) that may be more neurotoxic. In an Alzheimer's disease model, fibrillar A $\beta$  triggers dimerization of angiotensin II type 2 receptors (AT<sub>2</sub>) which becomes a substrate for TG2 and is further oligomerized (AbdAlla et al. 2009). AT<sub>2</sub> oligomerization results in sequestration of G $\alpha_{q/11}$  G protein which impairs M1 muscarinic receptor function. Excitotoxic neuronal cell death is an important component of acute injury in the CNS and also chronic neurodegenerative diseases. Tissue-specific overexpression of TG2 in mice sensitizes hippocampal neurons to apoptosis upon glutamate receptor overstimulation (Tucholski et al. 2006) and ischemic injury induces rapid upregulation of TG2 expression (Ientile et al. 2004) consistent with its regulation by acute-phase injury cytokines. A recent study provides evidence that TG2 has a broad effect on gene transcription by regulating chromatin structure through *N*-terminal polyamination of histone H3 in a model of HD and that TG2 inhibition protects striatal neurons from NMDA-mediated toxicity (McConoughey et al. 2010). Inflammation is a component of neurodegenerative diseases including HD and mediators such as TNF $\alpha$  may play a critical role in upregulating TG2 expression locally. Cytokine-mediated TG2 induction in astrocytes has been shown for acute spinal cord injury (Monsonogo et al. 1998) and MS lesions (van Strien et al. 2011). It has also become clear that there is significant complexity in the regulation of TG activity in the CNS. Two TG2 variants in addition to the full-length protein have been described in brain (Monsonogo et al. 1998; Citron et al. 2002; Antonyak et al. 2006; Tee et al. 2010). These result from alternative splicing, giving rise to truncated proteins essentially lacking either  $\beta$ -barrel 2 or both  $\beta$ -barrel domains and having unique short *C*-terminal sequences. Expression of these variants causes distinct changes in regulation of cell differentiation and survival as a consequence of differences in GTP binding of the variant proteins (Antonyak et al. 2006; Tee et al. 2010). Although the major contribution to TG activity in the CNS, and cerebral cortex in particular, has been ascribed to TG2 (Bailey and Johnson 2004),  $\gamma$ -glutamyl- $\epsilon$ -lysine crosslinks are formed in TG2-/- brain (Mastroberardino et al. 2002). Abundant expression of at least two other TG isozymes, TG1 and TG3, in the CNS has been shown (Kim et al. 1999), but the functional importance of this remains to be investigated. Here we characterize the hitherto uncharacterized TGM6 gene product and discuss it in the wider context of CNS development.

## Materials and methods

Detailed descriptions of experimental procedures are given in "Supplemental Material".

### Cell culture

H69 cells (American Type Culture Collection) were maintained as floating cell aggregates at a density of 6–30  $\times$  10<sup>4</sup> cells/ml in RPMI 1640 medium supplemented with 10% heat-inactivated foetal calf serum (FCS) containing 100 units/ml penicilin and 100  $\mu$ g/ml streptomycin. HEK293-EBNA cells were grown in DMEM:Ham's F-12 medium (1:1) supplemented with 10% FCS, 250  $\mu$ g/ml G418 (Invitrogen) and antibiotics. Neuro 2a cells (European Collection of Cell Cultures) were maintained in high-glucose DMEM supplemented with 10% FCS and antibiotics. For differentiation, cells were seeded at 5,000 cells/cm<sup>2</sup> in 24-well plates and stimulated for 3 days by reducing FCS to 0.5% and where indicated, adding 50 ng/ml NGF (Millipore), 1 mM dibutyryl cAMP (Sigma), or 10  $\mu$ M retinoic acid (Sigma).

### Cloning of human TG6

Overlapping fragments (corresponding to nucleotides 71–502, 409–876, 705–1,442, 1,369–1,720 and 1,666–2,292 in AF540969) of TG6 were amplified by RT-PCR from H69 poly(A)<sup>+</sup>RNA. The 5'-end of the cDNA was isolated by 5'-RACE PCR as described (Grenard et al. 2001) and the transcription initiation site determined by primer extension. A full-length cDNA for TG6 was constructed by subcloning the overlapping fragments as described (Hadjivassiliou et al. 2008). The full-length cDNA encoding TG6-L or TG6-S was subcloned into the pCEP-4 vector for expression in HEK293 EBNA cells (Smyth et al. 2000). Cell strains stably expressing TG6 were generated by transfection with lipofectamine (10  $\mu$ l for 2  $\mu$ g plasmid DNA) and selection with puromycin, starting with 0.5  $\mu$ g/ml puromycin after 48 h and gradually increasing to 10  $\mu$ g/ml over a 10 day period.

### Northern blotting

5  $\mu$ g of H69 cell poly(A)<sup>+</sup>RNA was separated in a 1.2% agarose gel, transferred to a nylon membrane and probed with a digoxigenin(DIG)-UTP-labelled single-stranded RNA probe corresponding to nucleotides 1,484–2,212 (AF540969) of TG6.

### Analysis of TG expression in mouse brain and cloning of mouse TG6

For cloning of mouse TG6, we prepared cDNA from BALB/c brain and used a series of gene-specific

oligonucleotides modelled from the human TG6 sequence to isolate overlapping DNA fragments by PCR. The 5'-end of the sequence was determined using 5'-RACE PCR and yielded besides the full-length mTG6 sequence a transcript with an alternative exon 1 (AY177607). Real-time PCR to quantify TG6 mRNA expression was carried out on an ABI 7700 Sequence Detection System using the 5' nuclease assay with primers 5'-CAGCAGTGGTAGGAGTGACAG (300 nM) and 5'-CTCTTGGAAGGGGTTATGTTG (600 nM) and labelled (5' 6-carboxyfluorescein and 3' 6-carboxytetramethylrhodamine) probe 5'-CAAGGACAGCTAAGTATTGAGGTGCCAG. Reaction conditions were as previously described except using 4 mM MgCl<sub>2</sub> (Stephens et al. 2004).

### Molecular modelling

A three-dimensional model of human TG6 was generated using ProMod II (version 3.70 SP3; Arnold et al. 2006) with the X-ray derived coordinates of human TG3 in its activated form (Protein Data Bank code 1L9N, chain A; Ahvazi et al. 2002) and the GDP-bound form of TG2 (1KV3, chain C; Liu et al. 2002) as a template resulting in final total energies of -32,300 and -17,400 kJ/mol, respectively, after optimizing the alignment manually.

### ELISA style transamidation assay

TG activity was determined by measurement of the incorporation of biotin-x-cadaverine (Molecular Probes) into *N,N*-dimethylcasein immobilized on the surface of protein binding 96-well plates essentially as described (Kleman et al. 1995).

### Real-time fluorescence assay for determination of TG isopeptidase activity

The effect of nucleotides on TG activity [human TG6 (T021; Zedira) or TG2] was quantified by measuring changes in fluorescence intensity over time at 37°C as a result of cleavage of Abz-APE( $\gamma$ -cad-Dnp)QEA (A102; Zedira) in the presence of different concentrations of GTP, GTP $\gamma$ S, GDP, GMP and ATP (Sigma). Fluorescence in the absence of enzyme activation (no Ca<sup>2+</sup>) was subtracted and reaction rates derived by linear regression. To obtain steady-state kinetics for the replacement reaction, acyl donor substrate concentration was varied from 3.2 to 170  $\mu$ M. Product concentration was derived from a concentration series of Abz-APQQEA. The kinetic parameters  $v_{\max}$  and  $K_M$  were obtained through nonlinear regression [ $v = (v_{\max} S)/(K_M + S)$ ] and  $k_{\text{cat}}$  calculated using  $k_{\text{cat}} = v_{\max}/E_0$ . All experiments were performed at least twice independently.

### In situ hybridization and immunolabelling of mouse tissue

Sagittal sections of adult BALB/c mouse brain or mouse embryos at different stages of gestation (E9–E16 and P0) were hybridized to DIG-labelled 325 bp sense and anti-sense RNA probes corresponding to the transcript region encoding the TG6  $\beta$ -barrels. Binding of the probes was detected using alkaline phosphatase-conjugated anti-DIG antibodies and visualized with NBT/BCIP. Polyclonal antibodies to TG6 were raised in goat against a peptide comprising residues 482–492 of mouse TG6 conjugated to hemocyanin (Hadjivassiliou et al. 2008) and affinity purified over a thiol Sepharose column bearing disulphide-linked peptide CGWRDDLLEPVTKPS as described (Aeschlimann and Paulsson 1991). The sequence of this loop connecting the catalytic core and  $\beta$ -barrel 1 domain is shared among all TG6 splice variants but highly divergent between different TGs. The absence of cross-reactivity with other TG isozymes was established (Hadjivassiliou et al. 2008). Immunolabelling for TG6 (1  $\mu$ g/ml) and  $\beta$ -tubulin III (Sigma T3952, 1:50 diluted) was performed as previously described using HRP-conjugated secondary antibodies and AEC (3-amino-9-ethyl carbazole) as a substrate (Aeschlimann et al. 1993).

### Isolation and differentiation of cortical progenitor cells

Cerebral cortex of newborn Balb/c mice was dissected on ice in Hanks' balanced salt solution (HBSS) and digested for 20 min at 37°C in 0.1% trypsin, 0.05% DNase I (Sigma) in HBSS. The tissue was washed and subsequently triturated in HBSS/DNase I solution to dissociate cells. Cells were washed and subsequently maintained in DMEM/F12 containing 2% B27 supplement (Invitrogen). Number of vital cells was determined by trypan blue exclusion. For FACS analysis, cells were washed in 0.5% BSA in phosphate-buffered saline, pH 7.4 (PBS), filtered through 40  $\mu$ m Falcon cell strainers (Becton–Dickinson) to remove remaining aggregates, fixed in 2% paraformaldehyde in PBS for 20 min on ice, permeabilized and stained with antibodies to TG6 (20  $\mu$ g/ml) and cell lineage markers, glial fibrillary acidic protein (G-A-5, Sigma; 15  $\mu$ g/ml),  $\beta$ -tubulin III (SDL.3D10, Sigma; 20  $\mu$ g/ml) and RIP (Chemicon, 1:1,000 diluted). For culture (formation of neurospheres), medium was supplemented with 20 ng/ml FGF2 (R&D Systems), 20 ng/ml EGF (Sigma) and antibiotics and  $1 \times 10^6$  cells seeded into 35 mm hydrophobic plastic dishes. For immunocytochemistry, cells were seeded at a density of  $1 \times 10^5$  cells/well in a 12-well plate on laminin-111 coated [purified from EHS tumour (Aeschlimann and Paulsson 1991)] cover slips and grown for 5 days. Cells were fixed in 4% paraformaldehyde,

permeabilized and labelled with antibodies to TG6 and cell lineage markers.

### Protein analysis

Protein concentrations were determined using the bicinchoninic acid reagent (Pierce) as described by the supplier with BSA as a standard. For immunoblotting, proteins were separated on 4–20% SDS–PAGE Tris–glycine gels under reducing conditions (1% 2-mercaptoethanol), transferred onto nitrocellulose membranes and stained with antibodies as described (Aeschlimann et al. 1993).

## Results and discussion

### TG6 cloning and primary structure

We have previously identified a cluster of TG genes in the human and mouse genome that contained a novel gene now termed TGM6 (Grenard et al. 2001). We used RT-PCR to screen different human cell lines for expression of the respective gene product. TG6 (previously called TG<sub>Y</sub>) could not be detected in cells of a wide variety of origins including mesenchymal, epithelial and hematopoietic cells suggesting that it has a restricted expression pattern, but its expression could be verified in a lung small cell carcinoma cell line, H69, both by RT-PCR and Northern blotting (Fig. 1a).

A full-length cDNA sequence for TG6 was obtained by PCR using oligo(dT) primed cDNA from H69 cells and a series of sequence specific primers based on the presumed transcribed genomic sequence (Supplemental Fig. 1). 5'-RACE PCR was used to identify the position of exon 1 which contains essentially non-coding sequence and therefore shows no apparent similarity between different TG genes. Primer extension was used to identify the 5'-end of the cDNA and this located the major transcription initiation site 455 nt upstream of the translation start codon (Supplemental Fig. 2). The likely 3'-end of the TG6 transcript may be inferred from an EST sequence in GenBank™ (AA961594). Based on this, a polyadenylation signal (ATAAA) could be located 3,887 nt downstream of the termination codon. This is preceded by a CFI<sub>m</sub>-binding site (TGTA) and followed by a GT-rich sequence known to bind CstF and therefore conforms to the tripartite element required for efficient 3' RNA processing (Venkataraman et al. 2005). The estimated size of the mRNA is therefore 6,480–6,490 nt which is in good agreement with the 6.3 kb transcript detected by Northern blotting (Fig. 1a). A prominent band at ~2.2 kb could indicate that a short transcript may also be abundant but the exact nature of that remains to be investigated. The obtained sequence

for full-length human TG6 contained an open reading frame of 2,120 nt. The deduced protein consists of 706 amino acids and has a calculated molecular mass of 79,276 Da. This mass is in good agreement with the size of the single protein band detected by Western blotting of keratinocyte protein extract (natively expressed protein) or when overexpressed in HEK293 cells after transfection with a TG6 expression construct (Fig. 1d). Recombinant enzyme displayed Ca<sup>2+</sup>-dependent transamidation activity (Fig. 1e).

A shorter transcript which apparently resulted from alternative splicing of the sequence encoded by exon 12 was also isolated from H69 cells (Fig. 1b). The absence of exon 12 results in a frame shift and thereby in premature termination within exon 13 (Supplemental Fig. 3). The sequence for the short form of TG6 (TG6-S) encoded a protein consisting of 625 amino acids ( $M_r$  70,480, calculated). The TG6-S sequence terminates just after the first C-terminal  $\beta$ -barrel domain and has a unique 14 amino acid C-terminus (Fig. 1c). Overexpression in HEK293 cells gives rise to a stable protein of expected size (Fig. 1d) suggesting that this alternative splicing event may have biological significance. The  $\beta$ -barrel domains have been implicated in the regulation of enzyme-substrate interaction and may also be involved in intracellular signalling as a sequence within the second  $\beta$ -barrel domain of TG2 is required for binding of PLC $\delta$ 1 (Hwang et al. 1995).

The H69 cell line displays neuronal characteristics including expression of neuron-specific enolase, brain isozyme of creatine kinase and L-dopa decarboxylase. We therefore reasoned that TG6 may be expressed in neurons. RT-PCR confirmed TG6 expression in mouse brain (see below). The cDNA sequence for mouse TG6 was isolated from brain, essentially using the same approach as for human (Supplemental Fig. 1). We have not determined the transcription initiation site. However, an EST sequence in GenBank™ (BY357397) derives from the genomic sequence upstream of the sequence we have isolated by RACE PCR indicating that transcription may be initiated at a position 389 nt upstream of the start codon, a position similar to that in the human gene in the aligned sequences. Two consecutive polyadenylation signals are present 1,096 nt downstream of the termination codon (Supplemental Fig. 1). Mouse and human TG6 have an 85% identity on the amino acid level.

Cloning identified two splice variants in mouse brain lacking either exon 3 or exon 3 together with exon 4 (Fig. 1c). Alternative splicing of exon 3 has been described by us and others for several TG genes including TG2, TG4, TG5 and band 4.2 protein and results in a TG with an altered N-terminal  $\beta$ -sandwich domain (Cohen et al. 1993; Aeschlimann et al. 1998; Candi et al. 2001; Cho et al. 2010; AK295775 in GenBank™). TG5 lacking exon 3 has

no transamidase activity (Candi et al. 2001). Omission of exon 3 and 4 results in a frame shift and premature termination before the sequence encoding the catalytic core domain, giving rise to a hypothetical 66 amino acid polypeptide without TG activity.

We could not detect alternative splicing of exon 12 in mouse brain or neuroblastoma cells. An identical sequence to H69 cell TG6-S was recently isolated from another cancer cell suggesting that this splice variant may be associated with oncogenic transformation. Four distinct C-terminally truncated versions of TG2 have been identified. Variants resulting from retention of intron 10 and 6, respectively, have been isolated from human disease states (Fraij et al. 1992; Citron et al. 2002). The former, TG2-S, results in a protein truncated within the sequence encoding  $\beta$ -barrel 1. Another TG2 short form resulting from splicing at an alternative 3' site within exon 12 and 5' acceptor site within exon 13 retains  $\beta$ -barrel 1 but has a distinct short C-terminal sequence (Monsonogo et al. 1998; Citron et al. 2002). This variant was originally identified in rat astrocytes, but similar variants, TG2-V1 and TG2-V2, resulting from use of two alternative 5' acceptor sites within exon 13 have subsequently been demonstrated in different human primary cells (Lai et al. 2007). However, in mouse brain no alternatively spliced variants of TG2 could be identified (Citron et al. 2005). Alternative splicing of exon 11 in human TG5 gives rise to a variant truncated within  $\beta$ -barrel 1 analogous to TG2-S (Candi et al. 2001). C-terminal truncation affects allosteric regulation of TG2 by GTP and has profound effects on cell differentiation and survival (Monsonogo et al. 1998; Antonyak et al. 2006; Tee et al. 2010).

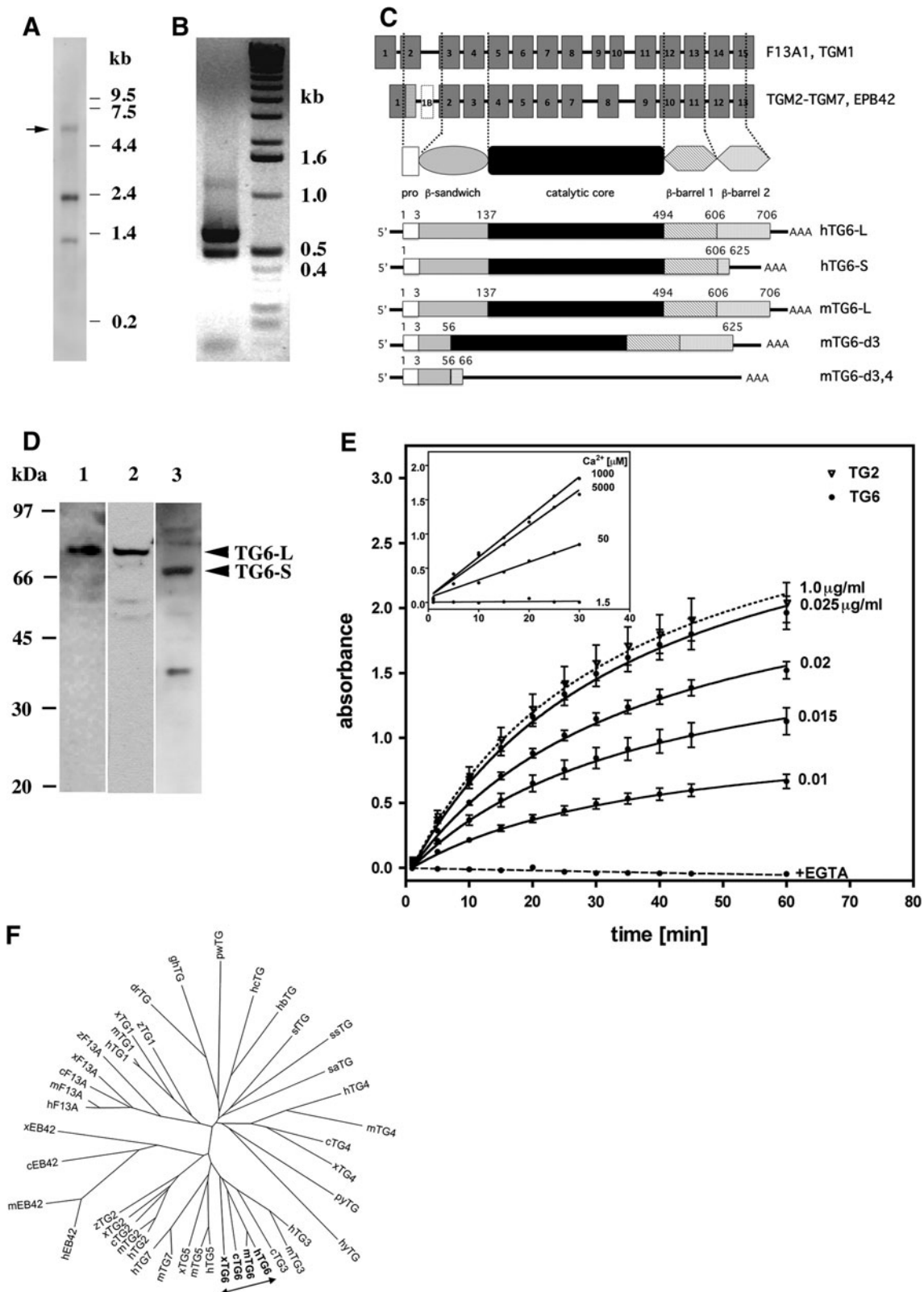
TG6 is a very low abundant transcript as indicated from directly analysing expression in specific cells and tissues as well as from whole genome expression profile studies. For mouse, the GenBank<sup>TM</sup> database contains a total of 21 independent ESTs. 18 of these are derived from skin and 1 each from retina and brain cortex. EST BB612839 is the splice variant lacking exon 3 and 4. For man, there is only a single EST from a lung small cell carcinoma. As a comparison, for TG2 the UniGene<sup>TM</sup> EST profile lists over 29,000 ESTs in normal human tissues alone.

#### TG6 origin in evolution

Alignment of TG sequences selected to represent major branches of animal evolution (Fig. 1f) indicates that the invertebrate and low chordata proteins are most closely related to the vertebrate isoforms TG4 and TG1. The factor XIII a-subunit derives from the same branch as TG1. The band 4.2 proteins show large divergence between species indicating low evolutionary pressure for conservation. In contrast to the mammalian and amphibian sequences, the

**Fig. 1** Analysis of human TGM6 gene products. **a** Size of transcripts expressed in H69 cells. Northern blot containing 5  $\mu$ g of poly(A<sup>+</sup>) RNA from H69 cells that was probed with a 0.7 kb antisense RNA corresponding to the two C-terminal  $\beta$ -barrel domains of TG6. The migration position of RNA size markers is indicated on the right and the full-length TG6 transcript with an arrow. **b** RT-PCR analysis identified two transcripts in H69 cells. PCR products spanning the relevant region of the transcript (left) were separated in a 1% agarose gel calibrated with the 1-kb ladder (right). These were identified by sequencing to result from alternative splicing of exon 12 (Supplemental Fig. 3). **c** Schematic illustrating the relationship between gene organization and protein structure in the TG family. TG4 contains an additional exon, exon 1B, within intron 1 (Cho et al. 2010) that can differentially be spliced in and encodes 45 amino acids. The band 4.2L variant contains an extended exon 1 (hatched box) (Sung et al. 1992). Variability in the 5' UTR has been reported in several TGM genes but does not alter the sequence of the protein encoded. Polyadenylated transcripts for TG6 isolated from H69 cells (hTG6) and mouse brain (mTG6) are shown underneath: L denotes full-length TG6, S TG6 lacking exon 12, d3 TG6 lacking exon 3 and d3,4 TG6 lacking exon 3 and 4. **d** Detection of TG6 in extracts of human keratinocytes (lane 1) or HEK293 cells transfected with hTG6-L (lane 2) or hTG6-S (lane 3) expression constructs by Western blotting. 10  $\mu$ g extracted protein was separated by SDS-PAGE under reducing conditions, transferred to nitrocellulose membranes and labelled with antibodies to TG6.  $M_r$  standards are indicated on the left. Keratinocytes express TG6-L but not TG6-S indicating that alternative splicing is cell-type dependent. **e** Transamidation activity of recombinant hTG6-L. The time-course for the incorporation of biotin-x-cadaverine into *N,N*-dimethylcasein with different concentrations of TG6 or TG2 was determined. Activity was Ca<sup>2+</sup>-dependent and maximal at [Ca<sup>2+</sup>] > 1 mM (data for TG6 shown in insert). The data are shown as mean  $\pm$  SD. **f** Protein sequence relationship of TGs. The dendrogram is based on a multiple sequence alignment of TGs including coagulation factor XIII a-subunit (F13A) and erythrocyte protein band 4.2 (EB42) from various species (*c* chicken, *h* human, *m* mouse, *x* frog, *Xenopus tropicalis*, *z* zebra fish, *Danio rerio*, *dr* fruit fly, *Drosophila melanogaster*, *hb* honey bee, *Apis mellifera*, *hc* horseshoe crab, *Tachypleus tridentatus*, *gh* grass hopper, *Schistocerca americana*, *hy* hydra, *Hydra magnipapillata*, *pw* pork worm, *Trichinella spiralis*, *py* *Physarum polycephalum*, *sa* sea anemone, *Nematostella vectensis*, *sf* starfish, *Asterina pectinifera*, *ss* sea squirt, *Ciona intestinalis*). The TG6 branches adjacent to TG3 are highlighted by an arrow. All sequences except for the human, mouse and frog band 4.2 protein contain the Cys, His and Asp residues of the catalytic triad

three reported avian band 4.2 sequences do contain the catalytic triad residues indicating that these proteins may function as active enzyme. Within the vertebrate TGs, the enzymatically inactive band 4.2 protein and TG2 form separate branches. The TG5/TG7 and TG3/TG6 pairs, each encoded by genes located closely together on the same chromosomes, are most closely related. A closer inspection reveals that the frog sequences marked xTG5 and xTG6 in Fig. 1f have ambivalent characteristics, and depending on the settings of alignment parameters could be also regarded as xTG7 and xTG3, respectively. Similarly, two bird sequences are predicted, which share characteristics of the TG5 and TG7 families. These data suggest that TG5/TG7 and TG3/TG6 arose from tandem gene duplication. We have previously proposed that two genome duplications in



early vertebrates may have given rise to ancestral TGM1, F13A1, TGMn and TGM4 genes and the ‘TGMn’ branch subsequently further specified through tandem duplication

to form the full complement of TG genes in mammals (TG2/3/5-7/EPB42; Grenard et al. 2001). The observation of four principle TG branches for the higher chordata is

consistent with the hypothesis of at least one whole genome duplication occurring after the urochordate ascidian *Ciona intestinalis*, as it has been proposed based on genome comparisons of ancestral vertebrates (Dehal and Boore 2005). More than one TG genes are also present in some protostome genomes. However, these appear to have arisen from gene duplication during protostome speciation independent from evolution of the TGM genes found in vertebrates.

#### TG6 architecture predicted by molecular modelling

Based on the high sequence similarity between TG6 and TG3 (overall sequence identity: 50 with 59% within the catalytic core domain), we used the high-resolution X-ray derived human TG3 structure (activated form with three bound calcium ions) as a template for generating a model of human TG6-L (Fig. 2a). The flexible solvent exposed loop, which is not resolved in the X-ray structure connects the last  $\alpha$ -helical region of the catalytic core to the first  $\beta$ -strand of the  $\beta$ -barrel 1 domain. The active site catalytic triad residues C274, H333 and D356 are at the base of a cavity, which is bound by the catalytic core and  $\beta$ -barrel 1 domains, and buried in a hydrophobic pocket, as in the case of TG3 (Fig. 2b). Consistent with biochemical data and the interpretation of the TG3 structure (Folk and Chung 1973; Ahvazi et al. 2002; Ahvazi and Steinert 2003), it can be assumed that the sulfhydryl group of C274 can form a thiolate-imidazolium ion pair with H333. The second nitrogen atom of the H333 ring is in hydrogen-bonding distance to the side chain oxygen atom of D356. The indole rings of the two tryptophan residues W238 and W330 are buried near the surface as in TG3 (W236, W327). It has been proposed that as a suitable glutamyl substrate approaches, an oxyanion intermediate forms with the former tryptophan, which results in break-down of the substrate to release  $\text{NH}_3$  and forms a thiol-acyl intermediate with the enzyme. This intermediate is attacked by the  $\epsilon$ -amine of a lysyl substrate to form another tetrahedral oxyanion intermediate with the latter tryptophan resulting in a cross-linked product (Pedersen et al. 1994). As in the TG3 structure, the corresponding hydroxyl oxygen of Y538 from the  $\beta$ -barrel 1 domain is within hydrogen-bonding distance of C274 and W238 and is located in the loop of the sequence motif I536–T539 that obstructs the entrance to the active site. The pair of serine residue S469/S470 in TG3, which serve as cleavage site for proteolytic activation by cathepsin L (Cheng et al. 2006), is not found in TG6 though cleavage by another enzyme cannot be ruled out. However, TG6 has a high specific activity in the absence of proteolytic processing (Fig. 1d). A redox-sensitive Cys switch that is involved in oxidative inactivation of TG2 through formation of a vicinal disulfide bond (Cys370–

Cys371) (Stamnaes et al. 2010a) is not replicated in TG6 in the same form as Cys230 is replaced by a serine residue. Nevertheless, TG6 is profoundly sensitive to oxidative inactivation.

#### Regulation of TG6 by co-factors

It is well established that transamidation activity of TGs requires binding of calcium ions (Folk and Chung 1973). As expected, activation of TG6 requires  $\text{Ca}^{2+}$ -binding and TG6 was found to display a similar concentration-dependence for activation as TG2 (Fig. 1e). In the case of factor XIII a, the activated enzyme contains a single calcium ion in a position near to the catalytic site (Fox et al. 1999) though its binding does not markedly alter the structure. For the zymogen form of TG3, a single tightly bound calcium ion has been found, but two further ions are bound upon proteolytic activation (Ahvazi et al. 2002). In our model of TG6, the highest affinity binding site 1 observed for TG3 is well conserved bringing the main chain carbonyl oxygen atoms of A223, N226, N228 and the side chain oxygens of N226, and D230 into coordinating distance of the TG3 inferred calcium ion position (Fig. 2c). A second calcium-binding site can be inferred to be formed by residues close to the C-terminal end of the catalytic core domain adjacent to the loop which joins the  $\beta$ -barrel 1 domain. The main chain oxygen atom of T417, and side-chain oxygens of N396, E445 and E450 are in a position to coordinate a calcium ion. In the case of TG3, calcium access to the related site in the zymogen form is hampered by the flexible loop (residues 462–471), which must be cleaved to allow entry. We do not yet know whether such a cleavage occurs in the case of TG6, though it could be speculated that the 11 residues longer loop might be more flexible to allow entry to this site, and this is supported by the high specific activity of the intact TG6 (Fig. 1e). A third calcium-binding site reported for activated TG3 is found adjacent to the catalytic triad histidine residue within a loop the position of which is shifted upon activation. The residues involved in calcium coordination are all conserved within the TG6 sequence and structural modelling suggests a corresponding orientation with the main chain carbonyl of S309 and side chain oxygen atoms of D303, D305, D327 and N307 as putative calcium acceptor sites.

It has been shown for TG2 (Achyuthan and Greenberg 1987; Im et al. 1990), TG3 (Boeshans et al. 2007) and TG5 (Candi et al. 2004) that enzymatic activity is inhibited by purine nucleotides.  $\text{Ca}^{2+}$ -binding and nucleotide binding occur at different sites and stabilize distinct conformations of TGs. The affinity of GTP is substantially reduced in the presence of extracellular  $\text{Ca}^{2+}$  concentrations allowing enzyme activation. In contrast to ATP, the affinity for GTP



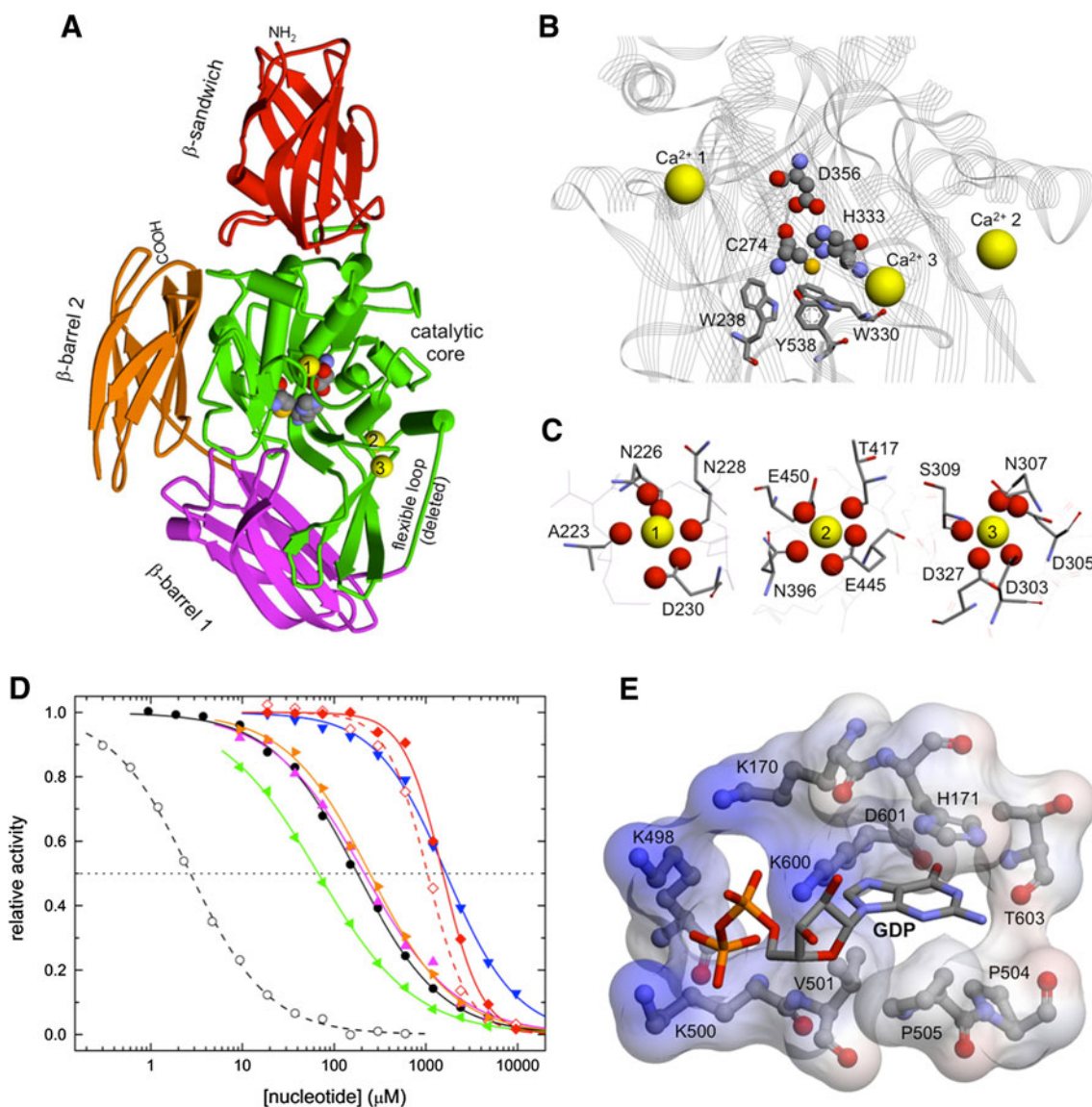


**Fig. 2** Model of the structure of human TG6-L and its interaction with nucleotides. **a** The overall structure as modelled based on the calcium activated TG3 form is shown. *Cylinders* and *arrows* denote  $\alpha$ -helical and  $\beta$ -strand conformations, respectively. The four domains ( $\beta$  sandwich, residues 3–136; catalytic core, res. 137–462;  $\beta$ -barrel 1, res. 494–605;  $\beta$ -barrel 2, res. 606–706) are depicted in different colours. The position of the three bound calcium ions of TG3 is shown by numbered *yellow spheres*. The residues of the catalytic triad are depicted in space-filling style. The flexible loop (res. 463–492) connecting the catalytic core with the  $\beta$ -barrel 1 domain has been deleted as the corresponding part is not resolved in the TG3 X-ray structure. **b** The residues of the catalytic triad and the adjacent tryptophan and tyrosine residues, the positions of which are proposed to be modulated by calcium (*yellow spheres*) binding, are shown as ball-and-stick and stick models, respectively. The side chain oxygen

of Y538 is in hydrogen-bonding distance to the sulphur atom of C274. **c** Oxygen atoms of TG6 residues, which are within 3.5 Å distance of the calcium ion sites of the TG3 template, are shown as *red spheres*. Further calcium coordination could arise from water molecules not included in the modelling. **d** Transamidation activity (measured as isopeptide replacement activity) of TG6 (*closed symbols; solid lines*) and TG2 (*open symbols, dashed lines*) was measured in the presence of various concentrations of nucleotides, and half-maximum activity is indicated by a *dotted line*: GTP, *black*; GTP in the presence of 1 mM  $Mg^{2+}$ , *orange*; GTP $\gamma$ S, *green*; GDP, *magenta*; GMP, *blue*; and ATP, *red*. *Symbols* indicate representative values of duplicate independent measurements. **e** The putative nucleotide-binding pocket was inferred from the GDP-bound TG2 structure. A semitransparent surface showing the electrostatic potential (*blue* positive, *red* negative) is overlaid over the residues surrounding a GDP molecule

and Mg-GTP is high and therefore of biological significance. Besides inhibiting transamidation activity intracellularly, independent functions of GTP binding and

hydrolysis in intracellular signalling have been proposed for TG2 (Im et al. 1990; Stephens et al. 2004; Iismaa et al. 2009).

We therefore determined the transamidation activity of TG6 in the presence of various nucleotides (Fig. 2d) using a quenched fluorescent substrate, Abz-APE( $\gamma$ -cad-Dnp)QEA, for real-time monitoring as suggested by Lorand and co-workers (Parameswaran et al. 1997). Folk's work has shown that the reaction occurs in a two-step mechanism whereby the active site thiol is transiently acylated by the  $\gamma$ -carboxamide group of the peptide-bound glutamine to form a stable acyl-enzyme intermediate. The second step involves either hydrolysis to convert Q to E or aminolysis by reaction with a primary amine to form the isopeptide bond and this is rate-limiting (Folk and Chung 1973). This reaction is reversible and steady-state kinetics can be performed by coupling isopeptide hydrolysis to a second reaction driven by an excess amine donor substrate. Given that the reactive nucleophilic form of the substrate is the neutral amine, maximum substrate conversion is achieved with amines deprotonated at physiological pH such as glycylmethylester or ethylene diamine ( $pK_a < 7$ ) (Leblanc et al. 2001). The sequence of the fluorescent substrate is based on the amine acceptor site of osteonectin/BM-40/SPARC for TG2 (Hohenadl et al. 1995). Nevertheless, the kinetic parameters given in Table 1 show that this peptide is a better substrate for TG6 than for TG2. When compared with TG2, a  $\sim 50$ -fold higher concentration of GTP (200  $\mu$ M) is required for half-maximal inhibition of TG6, whereas for ATP ( $\sim 1$  mM) similarly high concentrations are needed. The non-hydrolyzable GTP analogue GTP $\gamma$ S is a more effective inhibitor than GTP as has been reported for TG2 (Achyuthan and Greenberg 1987). Activity of TG6 is inhibited to a similar degree by GTP and GDP both in the absence and presence of 1 mM  $Mg^{2+}$ , but the affinity for GMP is low. Taken together, these data suggest that TG6 has the potential to function as a guanine nucleotide exchange factor in receptor signalling similar to TG2.

Based on the GDP-bound form of human TG2 (PDB code 1KV3, chain C, Liu et al. 2002), we modelled a putative corresponding nucleotide-binding pocket between the catalytic and  $\beta$ -barrel 1 domains (Fig. 2e). Such a TG6 GDP-binding site would be delineated by residues K170 and H171 from the catalytic domain, and K498 to P505 as well as K600 to E605 from the  $\beta$ -barrel 1 domain. The  $\epsilon$ -amino groups of lysine residues 170, 498, 500 and 600 envelop the phosphate groups of GDP, whereas V501–P505 and L604 surround the guanine group which is stacked by the imidazole ring of H171. In TG2, R478 and R580 form two ion pairs with the GDP  $\alpha$ - and  $\beta$ -phosphates. These residues are replaced by K500 and K600 in TG6. S482 and Y583 of TG2, which form hydrogen bonds with the N1 and N2 atoms of the guanine base are replaced by P505 and T603, respectively, in TG6 of which the main chain oxygen of T603 hydrogen bonds to N1 and N2, and

**Fig. 3** TG6 expression in mouse development. **a** Amplification of TGs from mouse whole brain cDNA. Products amplified with primers specific for TG1 (lane 1, 182 bp), TG2 (2, 177 bp), TG3 (3, 157 bp), TG5 (5, 135 bp), TG6 (6, 171 bp), and TG7 (7, 126 bp) could be detected but not TG4 (lane 4), factor XIII a-subunit (lane 8) and band 4.2 protein (lane 9). Products were analysed by electrophoresis in a 1% agarose gel calibrated with the 1-kb ladder. **b** TG6 expression in the developing and mature mouse brain. In situ hybridization was carried out with antisense (b) and sense (c) DIG-labelled TG6 RNA probes on serial sagittal sections of a newborn mouse or adult mouse brain (dark brown labelling with alkaline phosphatase and NBT/BCIP). A section stained with luxol fast blue/cresyl violet (a) shows the myelin and nuclei of nerve cells. C cortex, Cer cerebellum, ChP choroid plexus, Hip hippocampus, Mid mid brain, St striatum, Tha thalamus. Higher magnification images demonstrate labelling of cells in the cerebral cortex at P0 (d) and in mature brain (e) through layers II–VI, in Purkinje cells of the cerebellum (g) and keratinocytes in the epidermis and forming the hair shaft (h). Immunostaining of P0 serial section with antibodies recognizing the hinge region of TG6 confirms protein expression within the cell layers forming the motor cortex (red brown labelling with HRP and AEC) (f) and cells within grey matter of the spinal cord (FITC) (i). WM white matter, GM grey matter. **c** Sections of mouse embryo at the indicated developmental stages were hybridized with the antisense TG6 RNA probe. Images a–c depict a sagittal section through the developing head and images d–f a close-up of the telencephalon. A schematic illustrating the development of the cerebral cortex together with hematoxylin/eosin stained sections of the developing cerebral cortex at E11 and E16 is given in g. The cortical plate (CP) which will give rise to the multilayered neocortex (layers I–VI) develops between the marginal zone (MZ) and subplate (SP) which is derived from the preplate (PP). Pyramidal neurons within layer V/VI differentiate first and are positive for  $\beta$ -tubulin III by E16. Immunostaining for TG6 labels CP and layers V/VI of neocortex at E16 (g) whereas TG6 RNA expression is predominant in CP (f). IZ intermediate zone, SVZ subventricular zone, VZ ventricular zone

its oxygen to O6. Although the fold around a putative GDP molecule can be well adopted by TG6, the reduced number of interactions could be the cause for the observed decrease in nucleotide affinity (Fig. 2d).

#### Substrate specificity

There is a large degree of overlap in glutamine donor substrates of TG6, TG3, and TG2. On the level of fine specificity, however, clear differences exist. In peptides, TG2 has a highly sequence-dependent targeting (Gorman and Folk 1984; Vader et al. 2002; Hitomi et al. 2009), whereas TG6 shows tolerance to a broader spectrum of sequence changes in the neighbouring amino acids (Stamnaes et al. 2010b). The most significant influence on substrate properties is exerted by proline residues. None of the enzymes can modify glutamine residues directly followed by proline (-QP-), whereas proline at position +2 (-QXP-) exerts a positive influence. Furthermore, while all three enzymes readily target -PQ- sequences, proline in position -2 (-PPQ-) has a detrimental effect on recognition by TG2, but not TG6 or TG3. An indication that different positions may have a greater impact on

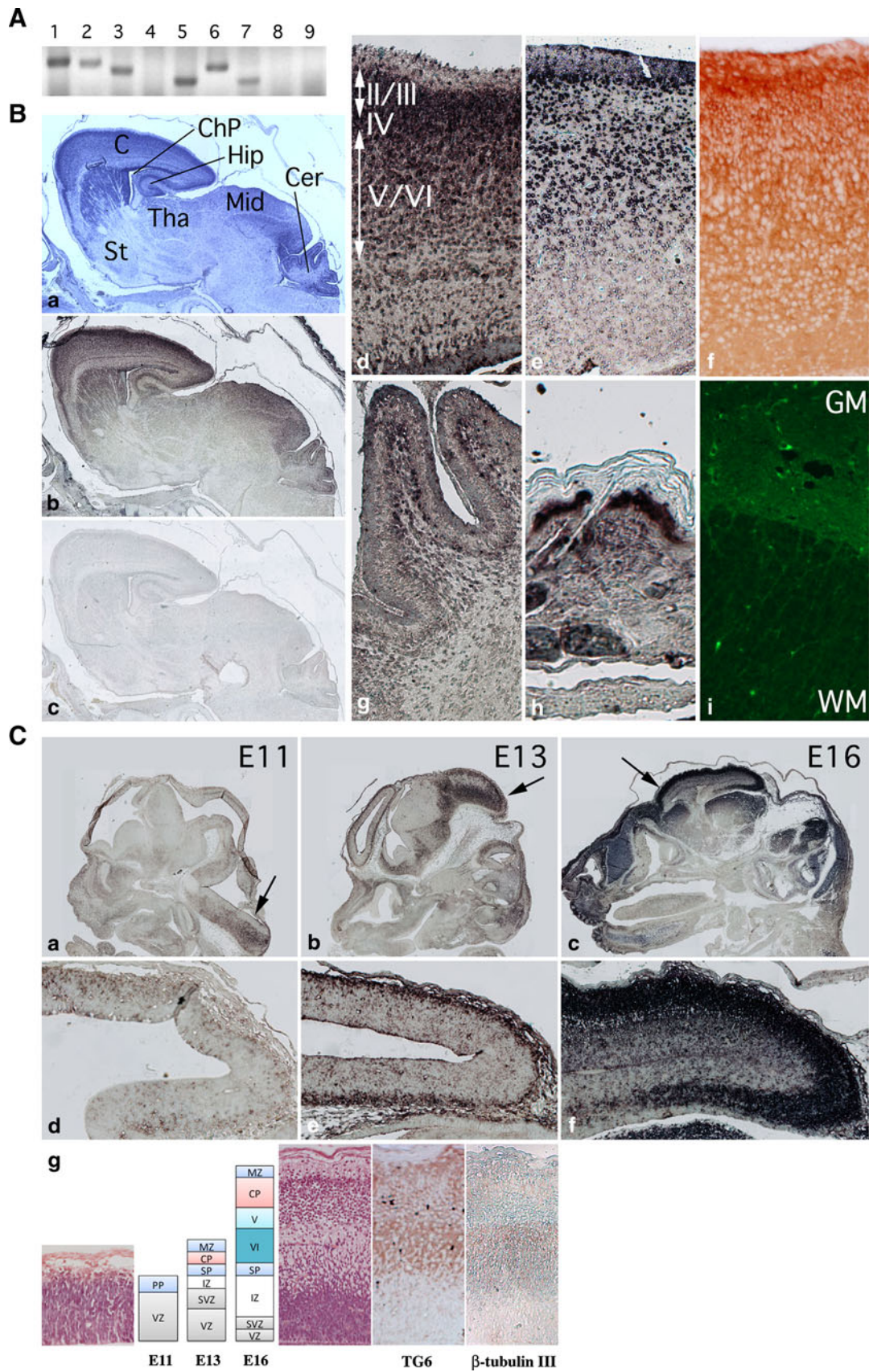


**Table 1** Kinetic parameters of TG2 and TG6 for the replacement reaction of Abz-APE( $\gamma$ -cad-Dnp)QEA at 37°C, pH 7.4, in the presence of an excess glycylmethylester

	$v_{\max}$ (M/s)	$k_{\text{cat}}$ (/s)	$K_M$ (M)	$k_{\text{cat}}/K_M$ (/M s)
TG2	$0.83 \pm 0.14 \times 10^{-9}$	$3.2 \pm 0.5 \times 10^{-3}$	$110 \pm 23 \times 10^{-6}$	$0.30 \pm 0.07 \times 10^2$
TG6	$2.6 \pm 0.4 \times 10^{-9}$	$10.1 \pm 1.6 \times 10^{-3}$	$49 \pm 12 \times 10^{-6}$	$2.1 \pm 0.6 \times 10^2$

Calculations were based on a molecular mass of 77 and 79 kDa for TG2 and TG6, respectively. The data are shown as mean  $\pm$  SD

substrate recognition by the different enzymes comes from the observed differences in relation to altered peptide length *N*- or *C*-terminal to the reactive glutamine residue. TG6 and TG2 are profoundly sensitive to the *C*-terminal sequence, whereas reactivity of TG3 with peptide substrates is primarily influenced by the sequence *N*-terminal to the glutamine residue (Stamnaes et al. 2010b). TG6 can both deamidate (Stamnaes et al. 2010b) and transamidate (Fig. 1d) glutamine residues, but it has not been determined yet for TG6 whether the type of modification that occurs preferentially is influenced by the sequence context as has been demonstrated for TG2 (Boros et al. 2006).

TG6 is associated with neuronal differentiation in the central nervous system

RT-PCR from mouse brain cDNA using specific primers for TG6 and also the other members of the TG family revealed expression of TG1, TG2, TG3, TG5, TG6 and TG7 (Fig. 3a). These results are consistent with demonstration of expression of TG1, TG2, TG3, and TG5 in the brain (Kim et al. 1999; Bailey and Johnson 2004; Bailey et al. 2004) and together with cell biological studies points to a highly complex regulation of TG genes in the CNS. To obtain a clearer understanding of TG6 expression on the cellular level, *in situ* hybridisation was performed on sagittal newborn mouse sections. An antisense RNA fragment corresponding to the *C*-terminal end of TG6 was used as a probe as this area has the least similarity between the different TGs and a similar human probe gave no cross-hybridisation with other TG gene products in Northern blotting. *In situ* hybridisation revealed that TG6 expression is widespread in the brain (Fig. 3b), most prominently within the cell layers containing the neuronal cell bodies of the cerebral cortex (particularly layers II–IV containing granular neurons and pyramidal cells) (image d), olfactory lobe (data not shown; see Fig. 3c, image c) and the cerebellum (Purkinje cells) (image g). TG6 expression was detected in the spinal cord (image i) and in the retinal cells of the eye (data not shown). TG6 was expressed in tissues other than the CNS, most prominently in the skin (image h) and other stratified squamous epithelia. Interestingly, these cells derive embryologically from a common ectodermal

progenitor. Immunolabelling with antibodies confirmed TG6 protein expression (image f).

Given the prominent expression of TG6 in the CNS in the developed organism, we were interested to identify whether the induction of TG6 expression correlated with any specific events in development. While the CNS is the first organ system to develop and to differentiate, it is also one of the last to be completed. The primary parts of the mouse brain can be identified soon after the neural groove, neural plate and head process stage at E7.5, and by day E14 has the typical anatomical layout of a mammalian brain. The neocortex is a highly organized six-layered structure that contains hundreds of different neuronal cell types and various subsets of glia. Progenitors residing in the ventricular zone produce the neurons of the different neocortical layers in a tightly controlled temporal order between about days E11 and E17.5 (Molyneaux et al. 2007). *In situ* hybridisation was therefore carried out on stage E11, E13 and E16 embryos (Fig. 3c). The walls of the primitive brain divide into an inner ependymal, an intermediate mantle, and outer marginal layer by E10, whereby the ependymal layer that ultimately forms the lining of the ventricles of the brain is the thickest layer. At E11, active proliferation of neuroblastic cells occurs in the walls of the entire CNS and these begin to occlude some of the neural cavities. Up to E11, the major neuroblastic activity is occurring behind the hindbrain where cranial ganglia V to IX develop. Little TG6 expression can be detected in the brain at E11 while labelling can be seen in the developing spinal cord (Fig. 3c, image a, arrow). By E13, TG6 expression is apparent in several parts of the brain and strong expression can now be detected in regions undergoing neuronal differentiation such as the mesencephalon (image b, arrow). From E13 to 16, the major neuroblastic activity occurs in the telencephalon where cells from the mantle layer migrate into the overlying marginal zone to form the neocortex which will become the outer grey matter of the cerebral hemispheres. At E13, TG6 expression is detected in a thin layer of the neocortex, presumably progenitor cells constituting the preplate (image e). By E16, TG6 is highly expressed in the outer layers of the neocortex (image f). TG6 mRNA expression is most prominent within the area of the cortical plate where neuronal differentiation occurs to form layers II–IV (image

f). TG6 protein is most prominent within layers V/VI where postmitotic neurons can be labelled for  $\beta$ -tubulin III at this stage (image g). Induction of TG6 expression appears to correlate both spatially and temporally with neurogenesis. In contrast, in situ hybridisation with a TG5 antisense RNA probe showed widespread expression throughout the CNS by E11 (data not shown).

Towards the latter stages of corticogenesis, astrocytes differentiate from radial glia. To clarify whether TG6 expression was associated with neurogenesis or astrocyte differentiation, progenitors were isolated from P0 stage mouse cortex and expanded in suspension culture as neurospheres (Murayama et al. 2002). To induce neuronal differentiation, progenitors were seeded on a laminin-111 substrate in the absence of mitogen for 5 days and subsequently labelled for TG6 and cell lineage markers. Cells of the neuronal lineage were identified using antibodies against  $\beta$ -tubulin III (Tuj-1), astrocytes with antibodies to glial fibrillary acidic protein (GFAP) and oligodendrocytes with RIP-antibodies (Sergent-Tanguy et al. 2003). Immunocytochemistry confirmed expression of TG6 in neuronal cells and its absence from the astroglial and oligodendroglial lineage (Fig. 4a). To exclude de novo expression of TG6 in neurons as a consequence of culture conditions, freshly isolated cells from the cerebral cortex of newborn mice were double-labelled with antibodies to TG6 and to the above cell lineage markers and analysed by FACS. 81% of cells were positive for TG6 and 58% for  $\beta$ -tubulin III, with 99% of  $\beta$ -tubulin III positive cells also positive for TG6. Physical parameters can be used to distinguish neurons, astrocytes and microglial cells as they differ in size and morphology (Sergent-Tanguy et al. 2003). Therefore, we plotted forward scatter (FSC), representing cell size, as a function of fluorescence intensity for TG6 labelling. Within the broad distribution of cells expressing TG6, two clusters of cells of different size were apparent and were gated (Supplemental Fig. 4, R1 and R2). Further analysis of gated cells for expression of cell lineage markers showed that both clusters were exclusively positive for  $\beta$ -tubulin III indicating that they are derived from the neuronal lineage and represent different neuronal populations (Supplemental Fig. 4).

Neuro2A is a mouse neural crest-derived cell line that has been extensively used to study neuronal differentiation, and specification into different neuronal lineages is possible (Tremblay et al. 2010). We initially confirmed that non-lineage-specific differentiation in low serum induced TG6 expression and subsequently used a number of differentiation factors to induce lineage-specific differentiation (Fig. 4b). Non-cholinergic differentiation with neurotrophin NGF was associated with strong upregulation of TG6. TG6 expression was also induced upon dopaminergic differentiation using dibutyryl cAMP,

whereas TG6 was not upregulated in cells treated with retinoic acid, a known inhibitor of dopaminergic differentiation. Quantitative PCR indicated that TG6 expression was upregulated twofold upon serum starvation and fourfold by dibutyryl cAMP. Dopamine neurons are formed in the olfactory lobe and retina during embryonic development, two areas where strong TG6 expression was seen in in situ hybridization (Fig. 3). However, the highest level of TG6 expression in Neuro 2a cells was observed upon induction of cell death by metal ion chelation suggesting that the strong TG6 expression observed during cerebral cortex development may relate in parts to association with programmed cell death rather than neuronal differentiation.

Cerebellar ataxia as consequence of genetic defects in TGM6 gene or acquired autoimmunity to TG6

Celiac disease (CD) is a common T cell-mediated autoimmune disorder characterized by its linkage to specific human lymphocyte antigen alleles, HLA-DQ2 and -DQ8 (Jabri and Sollid 2009). In susceptible individuals, consumption of gluten triggers a CD4<sup>+</sup> T-cell response to gliadin as well as a B cell response to gliadin and self antigens. TG2 contributes to disease development in at least two ways: first, by deamidating gluten peptides, thereby increasing their reactivity with HLA-DQ2/DQ8, which potentiates the T-cell response (Molberg et al. 1998; Van de Wal et al. 1998). Second, TG2 is the major autoantigen targeted by the B cell response (Dietrich et al. 1997). Although the T-cell response in the mucosa of the small intestine is the key player in disease development, gluten sensitivity is a systemic disease and autoantibodies may play a role in extraintestinal pathogenesis (Caja et al. 2011). This is supported by the recent demonstration of circulation derived anti-TG3 autoantibodies inducing a dermatitis herpetiformis-like pathology in human skin-grafted SCID mice (Zone et al. 2011). Neurological disorders have also been recognised as a form of extraintestinal manifestation of gluten sensitivity, with cerebellar involvement (gluten ataxia) and peripheral nerve involvement (gluten neuropathy) being the most common presentations (Hadjivassiliou et al. 2010). We have shown that gluten ataxia patients develop autoantibodies that are specific to TG6 (Hadjivassiliou et al. 2008). Furthermore, antibodies isolated from celiac disease patients are frequently reactive with human and mouse neurons. However, this neuronal reactivity is specific for antibodies that are crossreactive between the closely related TG2, TG3 and TG6 enzymes and is not mediated by TG2 as it is preserved in a TG2-/- background (Boscolo et al. 2010). This is consistent with TG2 being primarily associated with the vasculature in non-disease brain (Aeschlimann and

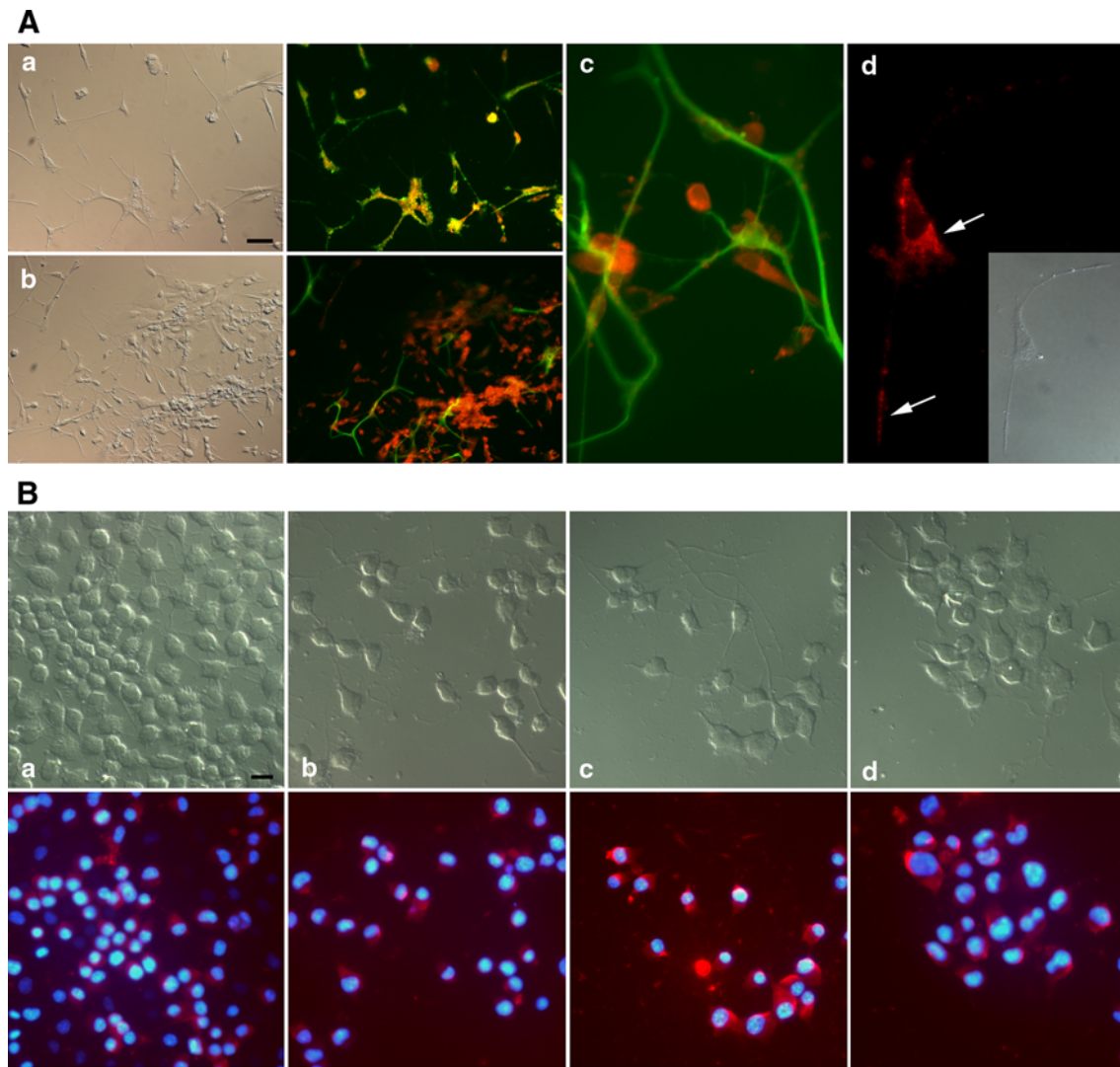


**Fig. 4 a** Confirmation of neurons as the primary source for TG6 expression in the mouse cerebral cortex. Progenitor cells from newborn mouse forebrain were grown as neurospheres and subsequently differentiated by culture in defined medium for 5 days on a laminin-111 substrate and double stained for TG6 (TRITC) and different cell markers (FITC):  $\beta$ -tubulin III isoform for neurons (a), GFAP for astrocytes (b, c). Co-expression of TG6 with  $\beta$ -tubulin III is highlighted by colour mixing (yellow, a). TG6 shows discrete subcellular distribution in large protein complexes or vesicles surrounding the nucleus and also in neurites (d, arrows). Left images in a, b and inset in d provide DIC images of the field of view shown

under fluorescence illumination. *Size bar* 40  $\mu$ m (a). **b** TG6 expression is upregulated concomitant with differentiation of Neuro 2a mouse neuroblastoma cells. Neuro 2a cells were grown with 10% FCS (a) or induced to differentiate by serum starvation (0.5% FCS) (b) or serum starvation in combination with NGF (50 ng/ml) (c) or dibutyryl cAMP (1 mM) (d) stimulation. After 3 days, cells were labelled with antibodies to TG6 (alexa fluor 568, bottom panels) and nuclei counterstained with Hoechst 34580. Upper panels provide DIC images of the field of view to illustrate changes in cell morphology. *Size bar* 10  $\mu$ m (a)

Paulsson 1991; Hadjivassiliou et al. 2008; Boscolo et al. 2010) and suggests that TG6 may be the neuronal autoantigen recognised in these patients. To test whether patient-derived autoantibodies directly contribute to pathology we attempted passive disease transfer. Serum immunoglobulin from gluten ataxia patients, as well as clonal anti-TG immunoglobulins derived using phage display, caused deficits in motor coordination but not anxiety

when injected intraventricularly in mice (Boscolo et al. 2010). The fact that isolated anti-TG immunoglobulins induce dramatic ataxia-like deficits in mice indicates selective neurotoxicity of anti-TG antibodies once exposed to the CNS and suggests that antibodies may play a role in disease transfer to the CNS. However, both scFv cross-reactive between different TGs and TG2-specific scFv compromised motor coordination in mice.

Cerebellar ataxias are a complex and heterogeneous group of neurodegenerative diseases characterized by progressive imbalance and limb movement deficits. About 20% of cerebellar ataxias display a familial inheritance pattern. So far, 30 different genetic loci have been linked to different SCA subtypes and 19 causative genes identified. Among those are CAG repeat expansion diseases including SCA1–3, 6–8, 12, 17, 31 and DRPLA and non-repeat mutations such as SCA 5, 11, 13–16, 27 and 28. A recent paper identified mutations in TGM6 in two Chinese families with autosomal dominant ataxia using linkage analysis and exome sequencing (Wang et al. 2010). Taken together with our demonstration of neuronal expression of TG6 and the presence of autoantibodies to TG6 in immune-mediated ataxia, this suggests that TG6 may play an important role in neurons involved in motor control. The mutations identified in TGM6 are single nucleotide exchanges leading to alteration of amino acid residues that are strictly conserved in TG6 among different species (D327G, L517W). Structural modelling suggests that the former substitution could interfere with  $\text{Ca}^{2+}$  binding at site 3 (Fig. 2c) and may therefore compromise enzyme activation, whereas the deleterious effect of the latter substitution remains obscure. It is also not clear why mutation of a single allele should produce a dominant ataxia phenotype. Haploinsufficiency is possible but one might also speculate that the problem is unrelated to the catalytic function and could be caused by difficulties in folding of mutant proteins and this may ultimately be neurotoxic. It is also interesting to note that alternative splicing or mutations in TG2 that affect its regulation by GTP have been shown to have dramatic effects on neuronal differentiation and to be pro-apoptotic in different cell types (Antonyak et al. 2006; Tee et al. 2010).

In order to gain a better understanding of the TG6-related pathology further work needs to address the physiological function of TG6 in the CNS. Given that TG6 similar to TG2 is a protein that can be detected in the cell cytosol as well as at the cell surface it may have independent intra- and extracellular functions that may employ the enzyme's ability to bind GTP or act as a  $\text{Ca}^{2+}$ -dependent crosslinking enzyme, respectively. Recent progress in the development of more isozyme-specific inhibitors may facilitate the elucidation of the context within which TG6 is activated and plays a critical role.

**Acknowledgments** We are grateful to Dr V. Pekarik for advice regarding the culture of primary neuronal progenitor cells. This study was supported by a grant from Coeliac UK and Arthritis Research UK (18461) and PhD studentships from Cardiff University to HT and MA. The nucleotide sequences reported in this paper have been deposited in the GenBank™/EBI Data Bank with the accession numbers AF540969 (full length) and AF540970 (exon 12 splice variant) for human TG6 and AY159126 (full length), AY177606

(exon 3/4 splice variant) and AY177607 (alternative exon 1) for mouse TG6.

**Open Access** This article is distributed under the terms of the Creative Commons Attribution Noncommercial License which permits any noncommercial use, distribution, and reproduction in any medium, provided the original author(s) and source are credited.

## References

- AbdAlla S, Lother H, el Missiry A, Langer A, Sergeev P, el Faraway Y, Quitterer U (2009) Angiotensin II  $\text{AT}_2$  receptor oligomers mediate G-protein dysfunction in an animal model of Alzheimer disease. *J Biol Chem* 284:6554–6565
- Achyuthan KE, Greenberg CS (1987) Identification of a guanosine triphosphate-binding site on guinea pig liver transglutaminase. *J Biol Chem* 262:1901–1906
- Aeschlimann D, Paulsson M (1991) Cross-linking of laminin-nidogen complexes by tissue transglutaminase. A novel mechanism for basement membrane stabilization. *J Biol Chem* 266:15308–15317
- Aeschlimann D, Paulsson M (1994) Transglutaminases: protein crosslinking enzymes in tissues and body fluids. *Thromb Haemost* 71:402–415
- Aeschlimann D, Thomazy V (2000) Protein crosslinking in assembly and remodelling of extracellular matrices: the role of transglutaminases. *Connect Tissue Res* 41:1–27
- Aeschlimann D, Wetterwald A, Fleisch H, Paulsson M (1993) Expression of tissue transglutaminase in skeletal tissues correlates with events of terminal differentiation of chondrocytes. *J Cell Biol* 120:1461–1470
- Aeschlimann D, Koeller MK, Allen-Hoffman BL, Mosher DF (1998) Isolation of a cDNA encoding a novel member of the transglutaminase gene family from human keratinocytes: detection and identification of transglutaminase gene products based on RT-PCR with degenerate primers. *J Biol Chem* 273:3452–3460
- Ahvazi B, Steinert PM (2003) A model for the reaction mechanism of the transglutaminase 3 enzyme. *Exp Mol Med* 35:228–242
- Ahvazi B, Kim HC, Kee SH, Nemes Z, Steinert PM (2002) Three-dimensional structure of the human transglutaminase 3 enzyme: binding of calcium ions changes structure for activation. *EMBO J* 21:2055–2067
- Ahvazi B, Boeshans KM, Rastinejad F (2004) The emerging structural understanding of transglutaminase 3. *J Struct Biol* 147:200–207
- Andringa G, Lam KY, Chegary M, Wang X, Chase TN, Bennett MC (2004) Tissue transglutaminase catalyzes the formation of alpha-synuclein crosslinks in Parkinson's disease. *FASEB J* 18:932–934
- Antonyak MA, Jansen JM, Miller AM, Ly TK, Endo M, Cerione RA (2006) Two isoforms of tissue transglutaminase mediate opposing cellular fates. *Proc Natl Acad Sci USA* 103:18609–18614
- Arnold K, Bordoli L, Kopp J, Schwede T (2006) The SWISS-MODEL Workspace: a web-based environment for protein structure homology modelling. *Bioinformatics* 22:195–201
- Bailey CD, Johnson GV (2004) Developmental regulation of tissue transglutaminase in the mouse forebrain. *J Neurochem* 91:1369–1379
- Bailey CD, Johnson GV (2005) Tissue transglutaminase contributes to disease progression in the R6/2 Huntington's disease mouse model via aggregate-independent mechanisms. *J Neurochem* 92:83–92
- Bailey CD, Graham RM, Nanda N, Davies PJ, Johnson GV (2004) Validity of mouse models for the study of tissue

- transglutaminase in neurodegenerative diseases. *Mol Cell Neurosci* 25:493–503
- Boeshans KM, Mueser TC, Ahvazi B (2007) A three-dimensional model of the human transglutaminase-1: insights into the understanding of lamellar ichthyosis. *J Mol Model* 13:233–246
- Boros S, Ahrman E, Wunderink L, Kamps B, de Jong WW, Boelens WC, Emanuelsson CS (2006) Site-specific transamidation and deamidation of the small heat-shock protein Hsp20 by tissue transglutaminase. *Proteins* 62:1044–1052
- Boscolo S, Lorenzon A, Sblattero D, Florian F, Stebel M, Marzari R, Not T, Aeschlimann D, Ventura A, Hadjivassiliou M, Tongiorgi E (2010) Anti-transglutaminase antibodies cause ataxia in mice. *PLOS ONE* 5:e9698 (1–9)
- Caja S, Mäki M, Kaukinen K, Lindfors K (2011) Antibodies in celiac disease: implications beyond diagnostics. *Cell Mol Immunol* 8:103–109
- Candi EG, Melino G, Mei G, Tarcsa E, Chung SI, Marekov LN, Steinert PM (1995) Biochemical, structural, and transglutaminase substrate properties of human loricrin, the major epidermal cornified cell envelope protein. *J Biol Chem* 270:26382–26390
- Candi E, Oddi S, Terrinoni A, Paradisi A, Ranalli M, Finazzi-Agró A, Melino G (2001) Transglutaminase 5 cross-links loricrin, involucrin, and small proline-rich proteins in vitro. *J Biol Chem* 276:35014–35023
- Candi E, Paradisi A, Terrinoni A, Pietroni V, Oddi S, Cadot B, Jogini V, Meiyappan M, Clardy J, Finazzi-Agro A, Melino G (2004) Transglutaminase 5 is regulated by guanine-adenine nucleotides. *Biochem J* 381:313–319
- Cheng T, Hitomi K, van Vlijmen-Willems IM, de Jongh GJ, Yamamoto K, Nishi K, Watts C, Reinheckel T, Schalkwijk J, Zeeuwen PL (2006) Cystatin M/E is a high affinity inhibitor of cathepsin V and cathepsin L by a reactive site that is distinct from the legumain-binding site. A novel clue for the role of cystatin M/E in epidermal cornification. *J Biol Chem* 281:15893–15899
- Cho SY, Choi K, Jeon JH, Kim CW, Shin DM, Lee JB, Lee SE, Kim CS, Park JS, Jeong EM, Jang GY, Song KY, Kim IG (2010) Differential alternative splicing of human transglutaminase 4 in benign prostate hyperplasia and prostate cancer. *Exp Mol Med* 42:310–318
- Citron BA, SantaCruz KS, Davies PJ, Festoff BW (2002) Intron-exon swapping of transglutaminase mRNA and neuronal Tau aggregation in Alzheimer's disease. *J Biol Chem* 276:3295–3301
- Citron BA, Zoloty JE, Suo Z, Festoff BW (2005) Tissue transglutaminase during mouse central nervous system development: lack of alternative RNA processing and implications for its role(s) in murine models of neurotrauma and neurodegeneration. *Brain Res Mol Brain Res* 135:122–133
- Cohen CM, Dotimas E, Korsgren C (1993) Human erythrocyte membrane protein 4.2 (pallidin). *Semin Hematol* 30:119–137
- Dehal P, Boore J (2005) Two rounds of whole genome duplication in the ancestral vertebrate. *PLOS Biol* 3:e314
- Dietrich W, Ehnis T, Bauer M, Donner P, Volta U, Riecken EO, Schuppan D (1997) Identification of tissue transglutaminase as the autoantigen of celiac disease. *Nat Med* 3:797–801
- Folk JE, Chung SI (1973) Molecular and catalytic properties of transglutaminases. *Adv Enzymol* 38:109–191
- Fox BA, Yee VC, Pedersen LC, Le Trong I, Bishop PD, Stenkamp RE, Teller DC (1999) Identification of the calcium binding site and a novel ytterbium site in blood coagulation factor XIII by x-ray crystallography. *J Biol Chem* 274:4917–4923
- Fraj BM, Birckbichler PJ, Patterson MK Jr, Lee KN, Gonzales RA (1992) A retinoic acid-inducible mRNA from human erythroleukemia cells encodes a novel tissue transglutaminase homologue. *J Biol Chem* 267:22616–22623
- Gorman JJ, Folk JE (1984) Structural features of glutamine substrate for transglutaminases. *J Biol Chem* 259:9007–9010
- Grenard P, Bates MK, Aeschlimann D (2001) Evolution of transglutaminase genes: identification of a gene cluster on human chromosome 15q15. Structure of the genes encoding transglutaminase X and a novel gene family member, transglutaminase Z. *J Biol Chem* 276:33066–33078
- Hadjivassiliou M, Aeschlimann P, Strigun A, Sanders D, Woodroffe N, Aeschlimann D (2008) Autoantibodies in gluten ataxia recognize a novel neuronal transglutaminase. *Ann Neurol* 64:332–343
- Hadjivassiliou M, Sanders DS, Grünewald RA, Woodroffe N, Boscolo S, Aeschlimann D (2010) Gluten sensitivity: from gut to brain. *Lancet Neurol* 9:318–330
- Hitomi K, Kitamura M, Sugimura Y (2009) Preferred substrate sequences for transglutaminase 2: screening using a phage-displayed peptide library. *Amino Acids* 36:619–624
- Hohenadl C, Mann K, Mayer U, Timpl R, Paulsson M, Aeschlimann D (1995) Two adjacent N-terminal glutamines of BM-40 (osteonectin, SPARC) act as amine acceptor sites in transglutaminase C-catalyzed modification. *J Biol Chem* 270:23415–23420
- Hwang KC, Gray CD, Sivasubramanian N, Im MJ (1995) Interaction site of GTP binding Gh (transglutaminase II) with phospholipase C. *J Biol Chem* 270:27058–27062
- Ientile R, Caccamo D, Marciano MC, Currò M, Mannucci C, Campisi A, Calapai G (2004) Transglutaminase activity and transglutaminase mRNA transcripts in gerbil brain ischemia. *Neurosci Lett* 363:173–177
- Iismaa SE, Mearns BM, Lorand L, Graham RM (2009) Transglutaminases and disease: lessons from genetically engineered mouse models and inherited disorders. *Physiol Rev* 89:991–1023
- Im MJ, Riek RP, Graham RM (1990) A novel guanine nucleotide-binding protein coupled to the  $\alpha 1$ -adrenergic receptor. II. Purification, characterization, and reconstitution. *J Biol Chem* 265:18952–18960
- Jabri B, Sollid LM (2009) Tissue-mediated control of immunopathology in coeliac disease. *Nat Rev Immunol* 9:858–870
- Jeitner TM, Matson WR, Folk JE, Blass JP, Cooper AJ (2008) Increased levels of gamma-glutamylamines in Huntington disease CSF. *J Neurochem* 106:37–44
- Jeitner TM, Muma NA, Battaile KP, Cooper AJ (2009) Transglutaminase activation in neurodegenerative diseases. *Future Neurol* 4:449–467
- Kim SY, Grant P, Lee JH, Pant HC, Steinert PM (1999) Differential expression of multiple transglutaminases in human brain. Increased expression and cross-linking by transglutaminases 1 and 2 in Alzheimer's disease. *J Biol Chem* 274:30715–30721
- Kleman JP, Aeschlimann D, Paulsson M, van der Rest M (1995) Transglutaminase-catalyzed cross-linking of fibrils of collagen V/XI in A204 rhabdomyosarcoma cells. *Biochemistry* 34:13768–13775
- Lai TS, Tucker T, Burke JR, Strittmatter WJ, Greenberg CS (2004) Effect of tissue transglutaminase on the solubility of proteins containing expanded polyglutamine repeats. *J Neurochem* 88:1253–1260
- Lai TS, Liu Y, Li W, Greenberg CS (2007) Identification of two GTP-independent alternatively spliced forms of tissue transglutaminase in human leukocytes, vascular smooth muscle, and endothelial cells. *FASEB J* 21:4131–4143
- Leblanc A, Gravel C, Labelle J, Keillor JW (2001) Kinetic studies of guinea pig liver transglutaminase reveal a general-base-catalyzed deacylation mechanism. *Biochemistry* 40:8335–8342
- Lesort M, Chun W, Johnson GV, Ferrante RJ (1999) Tissue transglutaminase is increased in Huntington's disease brain. *J Neurochem* 73:2018–2027



- Liu S, Cerione RA, Clardy J (2002) Structural basis for the guanine nucleotide-binding activity of tissue transglutaminase and its regulation of transamidation activity. *Proc Natl Acad Sci USA* 99:2743–2747
- Lorand L, Graham RM (2003) Transglutaminases: crosslinking enzymes with pleiotropic functions. *Nat Rev Mol Cell Biol* 4:140–156
- Mariani P, Carsughi F, Spinozzi F, Romanzetti S, Meier G, Casadio R, Bergamini CM (2000) Ligand-induced conformational changes in tissue transglutaminase: Monte Carlo analysis of small-angle scattering data. *Biophys J* 78:3240–3251
- Mastroberardino PG, Iannicola C, Nardacci R, Bernassola F, De Laurenzi V, Melino G, Moreno S, Pavone F, Oliverio S, Fesus L, Piacentini M (2002) ‘Tissue’ transglutaminase ablation reduces neuronal death and prolongs survival in a mouse model of Huntington’s disease. *Cell Death Differ* 9:873–880
- McConoughey SJ, Basso M, Niatsetskaya ZV, Sleiman SF, Smirnova NA, Langley BC, Mahishi L, Cooper AJ, Antonyak MA, Cerione RA, Li B, Starkov A, Chaturvedi RK, Beal MF, Coppola G, Geschwind DH, Ryu H, Xia L, Iismaa SE, Pallos J, Pasternack R, Hils M, Fan J, Raymond LA, Marsh JL, Thompson LM, Ratan RR (2010) Inhibition of transglutaminase 2 mitigates transcriptional dysregulation in models of Huntington disease. *EMBO Mol Med* 2:349–370
- Molberg O, Mcadam SN, Körner R, Quarsten H, Kristiansen C, Madsen L, Fugger L, Scott H, Norén O, Roepstorff P, Lundin KE, Sjöström H, Sollid LM (1998) Tissue transglutaminase selectively modifies gliadin peptides that are recognized by gut-derived T cells in celiac disease. *Nat Med* 4:713–717
- Molyneaux BJ, Arlotta P, Menezes JRL, Macklis JD (2007) Neuronal subtype specification in the cerebral cortex. *Nat Rev Neurosci* 8:427–437
- Monsonogo A, Friedmann I, Shani Y, Eisenstein M, Schwartz M (1998) GTP-dependent conformational changes associated with the functional switch between Galpha and cross-linking activities in brain-derived tissue transglutaminase. *J Mol Biol* 282:713–720
- Murayama A, Matsuzaki Y, Kawaguchi A, Shimazaki T, Okano H (2002) Flow cytometric analysis of neural stem cells in the developing and adult mouse brain. *J Neurosci Res* 69:837–847
- Nemes Z, Devreese B, Steinert PM, Van Beeumen J, Fésüs L (2004) Cross-linking of ubiquitin, HSP27, parkin, and alpha-synuclein by gamma-glutamyl-epsilon-lysine bonds in Alzheimer’s neurofibrillary tangles. *FASEB J* 18:1135–1137
- Parameswaran KN, Cheng XF, Chen EC, Velasco PT, Wilson JH, Lorand L (1997) Hydrolysis of gamma:epsilon isopeptides by cytosolic transglutaminases and by coagulation factor XIIIa. *J Biol Chem* 272:10311–10317
- Pedersen LC, Yee VC, Bishop PD, Le Trong I, Teller DC, Stenkamp RE (1994) Transglutaminase factor XIII uses proteinase-like catalytic triad to crosslink macromolecules. *Protein Sci* 3:1131–1135
- Pinkas DM, Strop P, Brunger AT, Khosla C (2007) Transglutaminase 2 undergoes a large conformational change upon activation. *PLoS Biol* 5:e327
- Sergent-Tanguy S, Chagneau C, Neveu I, Naveilhan P (2003) Fluorescent activated cell sorting (FACS): a rapid and reliable method to estimate the number of neurons in a mixed population. *J Neurosci Methods* 129:73–79
- Smyth N, Odenthal U, Merkl B, Paulsson M (2000) Eukaryotic expression and purification of recombinant extracellular matrix proteins carrying the Strep II tag. *Methods Mol Biol* 139:49–57
- Stamnaes J, Pinkas DM, Fleckenstein B, Khosla C, Sollid LM (2010a) Redox regulation of transglutaminase 2 activity. *J Biol Chem* 285:25402–25409
- Stamnaes J, Dorum S, Fleckenstein B, Aeschlimann D, Sollid LM (2010b) Gluten T-cell epitope targeting by TG3 and TG6; implications for dermatitis herpetiformis and gluten ataxia. *Amino Acids* 39:1183–1191
- Stephens P, Grenard P, Aeschlimann P, Langley M, Blain E, Errington R, Kipling D, Thomas D, Aeschlimann D (2004) Crosslinking and G-protein functions of transglutaminase 2 contribute differentially to fibroblast wound healing responses. *J Cell Sci* 117:3389–3403
- Sung LA, Chien S, Fan YS, Lin CC, Lambert K, Zhu L, Lam JS, Chang LS (1992) Erythrocyte protein 4.2: isoform expression, differential splicing, and chromosomal assignment. *Blood* 79:2763–2770
- Tee AE, Marshall GM, Liu PY, Xu N, Haber M, Norris MD, Iismaa SE, Liu T (2010) Opposing effects of two tissue transglutaminase protein isoforms in neuroblastoma cell differentiation. *J Biol Chem* 285:3561–3567
- Tremblay RG, Sikorska M, Sandhu JK, Lanthier P, Ribocco-Lutkiewicz M, Bani-Yaghoob M (2010) Differentiation of mouse Neuro 2A cells into dopamine neurons. *J Neurosci Methods* 186:60–67
- Tucholski J, Roth KA, Johnson GV (2006) Tissue transglutaminase overexpression in the brain potentiates calcium-induced hippocampal damage. *J Neurochem* 97:582–594
- Vader LW, de Ru A, van der Wal Y, Kooy YM, Benckhuijsen W, Mearin ML, Drijfhout JW, van Veelen P, Koning F (2002) Specificity of tissue transglutaminase explains cereal toxicity in celiac disease. *J Exp Med* 195:643–649
- van de Wal Y, Kooy Y, van Veelen P, Peña S, Mearin L, Papadopoulos G, Koning F (1998) Selective deamidation by tissue transglutaminase strongly enhances gliadin-specific T cell reactivity. *J Immunol* 161:1585–1588
- van Strien ME, Drukarch B, Bol JG, van der Valk P, van Horsen J, Gerritsen WH, Breve JJ, van Dam AM (2011) Appearance of tissue transglutaminase in astrocytes in multiple sclerosis lesions: a role in cell adhesion and migration? *Brain Pathol* 21:44–54
- Venkataraman K, Brown KM, Gilmartin GM (2005) Analysis of a noncanonical poly(A) site reveals a tripartite mechanism for vertebrate poly(A) site recognition. *Genes Dev* 19:1315–1327
- Wang JL, Yang X, Xia K, Hu ZM, Weng L, Jin X, Jiang H, Zhang P, Shen L, Guo JF, Li N, Li YR, Lei LF, Zhou J, Du J, Zhou YF, Pan Q, Wang J, Wang J, Li RQ, Tang BS (2010) *TGM6* identified as a novel causative gene of spinocerebellar ataxias using exome sequencing. *Brain* 133:3510–3518
- Yee VC, Pedersen LC, Le Trong I, Bishop PD, Stenkamp RE, Teller DC (1994) Three-dimensional structure of a transglutaminase: human blood coagulation factor XIII. *Proc Natl Acad Sci USA* 91:7296–7300
- Zainelli GM, Ross CA, Troncoso JC, Muma NA (2003) Transglutaminase cross-links in intranuclear inclusions in Huntington disease. *J Neuropathol Exp Neurol* 62:14–24
- Zone JJ, Schmidt LA, Taylor TB, Hull CM, Sotiriou MC, Jaskowski TD, Hill HR, Meyer LJ (2011) Dermatitis herpetiformis sera or goat anti-transglutaminase-3 transferred to human skin-grafted mice mimics dermatitis herpetiformis immunopathology. *J Immunol* 186:4474–4480